Atomic scale surface structure and morphology of InAs nanowire crystal superlattices: The effect of epitaxial overgrowth

J. Knutsson[1], S. Lehmann[1], M. Hjort[1], P. Reinke[2], E. Lundgren[1], K.A. Dick[1,3], R. Timm[1] and A. Mikkelsen[1*

[1]*Department of Physics, Lund University, P.O. Box 118, 22 100 Lund, Sweden*

[2] *Department of Materials Science and Engineering, University of Virginia, 395 McCormick Road, Charlottesville, Virginia 22904, USA*

[3]*Department of Chemistry, Lund University, P.O. Box 124, 221 00 Lund, Sweden*

e-mail: anders.mikkelsen@sljus.lu.se

Stage V

In stage V, see Figure S1, no well-defined remnants of the {111}A/B facets can be seen. Only a rough unordered surface remains (edges in the image) approximately corresponding to {112} type planes.
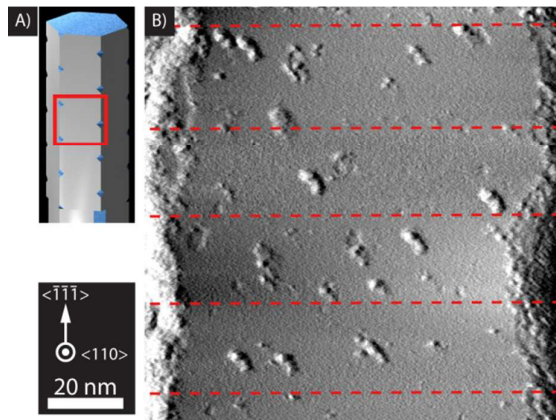
Figure S1: *STM image of a Zb segment in stage V. Red dashed lines denote twin plane positions. The image has been differentiated to make the height variations more clearly visible. U=−1.0 V, I=50 pA*

Nonlinear growth rate

When imaging the {111}A/B facets along TSL segments, it was found that the overgrowth was not constant over time, but rather accelerated as time progressed. Such acceleration could be caused by a non-linear nucleation rate, i.e. the time between nucleation events at the twin plane of the concave interface decrease over time resulting in new layers forming more and more rapidly, or due to a material limited growth. A non-constant nucleation rate can be ruled out as it would give rise to a non-linear growth of the {110} facet, but a linear growth of the {110} facet width was measured, see Figure S2. The width of the {110} facets, the depths of the V-groove pockets as well as widths of the concave interface were measured for several grooves, interfaces and twin boundaries along a top Zb segment. They all show a linear trend with respect to distance from the Au-particle, i.e. overgrowth time, indicating that the rate of forming overgrowth layers on the facets must have been constant along the NW, and thus over time. This suggests that a limitation in material supply is causing the non-linearity in the growth rate.
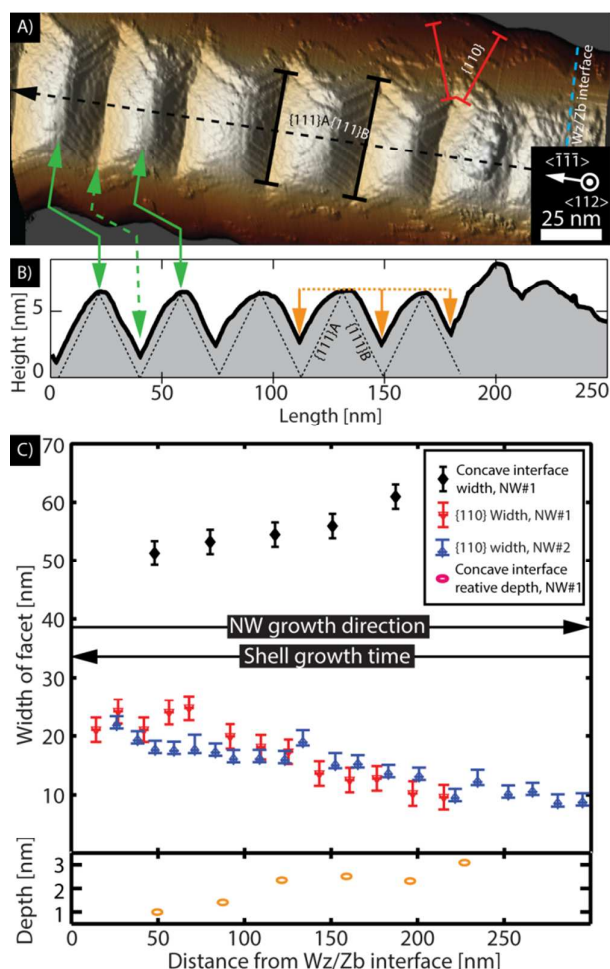

***Figure* S2:** *(A) STM image represented in 3D of a top Zb segment seen from a <112> direction. The convex and concave {111}A/B interfaces are marked with solid and dashed (both green) arrows respectively. Solid black and red lines illustrate how the width of the concave interface line and the width of the {110} facet was measured respectively. Dashed light blue line denotes the Wz/Zb interface. U=−1.0 V, I=50 pA. (B) Line profile along*

[−1−1−1] direction of the Zb segment, as marked by black dashed arrow in figure (A). Yellow arrows illustrate how the depths of the V-groove pockets were measured. (C) Plot of the width of {110} facet (red for NW 1 and blue for NW 2) and width of concave {111}A/B interface of NW 1(black) as a function of distance from the Wz/Zb interface. Error bars show estimated error when measuring facet width. Sub-plot (pink) shows relative depth of concave interface of NW 1 as indicated by yellow arrows in the line profile of figure (B).

Growth rate vs. Nucleation rate on {111}B

A ratio between the step flow growth of a triangle shaped overgrowth layer and the nucleation rate along the {111}A/B interface line can be roughly estimated by assuming that the size of a triangle is correlated with the time of nucleation of that layer, meaning that a large triangle nucleated before a smaller one, i.e. triangle N1 in figure S3 nucleated before triangle N2, N3 and N4. This in turn assumes that the growth rate is the same for all step edges during a time scale corresponding to a few nucleation events. Measuring the distance from the nucleation site at the interface to the step edge of a triangle along the <111>B directions, see Figure S3, an estimate of how far this step edge has grown since its nucleation time can be obtained. By comparing such measurements from triangles which nucleated after each other, an estimate of how far a step edge grows in between two nucleation events is obtained. This calculation gives that a step edge grows roughly 2.0 nm, with a standard deviation of 1.9 nm, before a new nucleation event occurs along the interface.
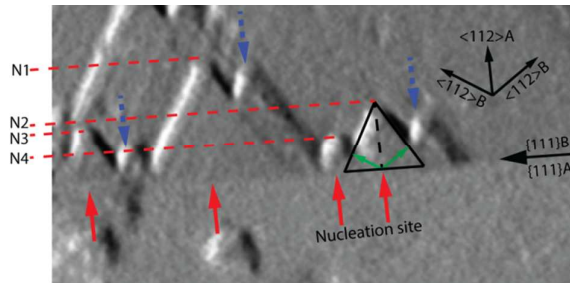
***Figure* S3:** *STM image of {111}A/B interface. The image has been differentiated to make the height variations more clearly visible. Red arrows denote nucleation sites of triangle shaped layers. Blue dashed arrows denote triangles that are not "real", but an artifact of a "double tip". Green arrows illustrate how the distance from a nucleation site to a step edge was measured. Red dashed lines indicate the relative size of the different triangles. U=−1.7 V, I=100 pA.*

The effects of hydrogen cleaning

During transport in air (from the MOVPE growth reactor to the STM) the NW surfaces will form a thin layer of native oxide. In order to study oxide-free NW surfaces, a cleaning procedure was performed by annealing the samples to 380 ℃ in an atomic hydrogen atmosphere with a pressure of $2 \cdot 10^{-6}$ mbar for 20–40 min. A relevant point is to which degree of accuracy the morphology of the as grown nanowires is retained. The oxidation that InAs NWs (and planar surfaces) experience upon exposure to air has been studied in detail by X-ray photoelectron spectroscopy (XPS) [1]. This shows that the native oxide formed on these nanowires is ~10Å, which is even less than on corresponding planar substrates. Since the density of As and In in the oxide is less than in pure InAs, this indicates that only very few

atomic layers are dissolved in the oxide. This is also corroborated by TEM measurements of similar type of NWs, which show that the surface oxide must be very thin and homogeneous [2-4]. This is indicative of a homogeneous self-limited native oxide growth on InAs nanowires (as is also found on planar surfaces). This is also consistent with only very small changes in the NW oxide thickness even after exposures to ambient air for months.

The next relevant question is then the effect of the hydrogen cleaning on the nanowires. During STM characterization, we have to perform new cleaning procedures of the nanowires regularly; this is mainly because they start to re-oxidize after some days in the STM due to the presence of small amounts of Oxygen and water in the STM chamber. Our re-cleaning procedures results in no changes of the atomic scale structure and morphology of the nanowires as we could see from measurements of several nanowires before and after. To further directly investigate the influence of the oxidation/reduction on the nanowire morphology, it is highly useful to do experiments where nanowires have been initially cleaned and their morphology determined by STM, whereupon the same sample of nanowires have been exposed to ambient air for 30min or longer and then re-cleaned. We have on some occasions transferred the same InAs NW sample in and out of vacuum and thus re-cleaned wires to perform such experiments. From these measurements we know that the Oxidation and hydrogen cleaning does not change the overall morphology of the InAs nanowires and results in no new atomic scale reconstructions on the surface.

To further ensure that the original cleaning did not cause major changes we have checked that the STM image profiles, of hydrogen cleaned InAs NWs, projected along the directions of TEM images of similar NWs are identical to the profiles observed in the TEM images.

While a homogeneous Oxidation followed by a homogeneous Oxide removal can leave the surface rather untouched, we should also be able to find cases where the Oxidation makes a difference. So to further investigate the influence of oxidation and hydrogen cleaning on the atomic-scale surface structure, we have also performed so called cross-sectional STM (XSTM) experiments [5]. By cleaving an InAs(001) substrate in vacuum, a clean and well-defined InAs(110) surface is obtained. The cleaved sample is defect free except for occasional steps; the surface has the same unreconstructed atomic structure as found on the nanowires [6]. First, the cleaved sample is cleaned in atomic hydrogen following the same procedure as used for the NWs. This results in exactly the same type of atomic scale and step structure as prior to the cleaning. The sample was then exposed to ambient air for 30 min followed by a hydrogen cleaning procedure as described above. This still leaves the original step structure intact to the level of a few atomic rows, however on larger terraces one can also note a formation of small single monolayer islands with a diameter of 10-20nm.These islands are not observed in areas with high step density, as would be the case for nanowires with diameters as found in the present study. They are also not observed on the (110) terraces of the nanowires of the present study. Their origin is presumably due to the regrowth of InAs from the Oxide occurring on the large terraces and will be discussed in detail elsewhere [7].

References

(1) Timm, R.; Hjort, M.; Fian, A.; Borg, B.M.; Thelander, C.; Andersen, J.N.; Wernersson, L.-E., and Mikkelsen, A., Interface Composition of Inas Nanowires with Al2o3 and Hfo2 Thin Films. *Applied Physics Letters,* **2011**. 99, -.

(2) Dick, K.A.; Thelander, C.; Samuelson, L., and Caroff, P., Crystal Phase Engineering in Single Inas Nanowires. *Nano Letters,* **2010**. 10, 3494-3499.

(3) Bolinsson, J.; Caroff, P.; Mandl, B., and Dick, K.A., Wurtzite-Zincblende Superlattices in Inas Nanowires Using a Supply Interruption Method. *Nanotechnology,* **2011**. 22.

(4) Xu, T.; Dick, K.A.; Plissard, S.; Nguyen, T.H.; Makoudi, Y.; Berthe, M.; Nys, J.P.; Wallart, X.; Grandidier, B., and Caroff, P., Faceting, Composition and Crystal Phase Evolution in Iii-V Antimonide Nanowire Heterostructures Revealed by Combining Microscopy Techniques. *Nanotechnology,* **2012**. 23, 095702.

(5) Yu, E.T., Cross-Sectional Scanning Tunneling Microscopy. *Chemical Reviews,* **1997**. 97, 1017-1044.

(6) Hjort, M.; Lehmann, S.; Knutsson, J.; Zakharov, A.A.; Du, Y.A.; Sakong, S.; Timm, R.; Nylund, G.; Lundgren, E.; Kratzer, P.; Dick, K.A., and Mikkelsen, A., Electronic and Structural Differences between Wurtzite and Zinc Blende Inas Nanowire Surfaces: Experiment and Theory. *ACS Nano,* **2014**. 8, 12346-12355.

(7) Hjort, M.; Knutsson, J.; Mandl, B.; Timm, R.; Lundgren, E.; Deppert, K., and Mikkelsen, A., Manuscript in Preparation.